Isotopic Ratios of Saturn's Rings and Satellites: Implications for the Origin of Water and Phoebe

By

Roger N. Clark[1], Robert H. Brown[2], Dale P. Cruikshank[3], and Gregg A. Swayze[4]

[1]Planetary Science Institute, 1700 East Fort Lowell, Suite 106, Tucson, AZ 85719-2395, USA
 rclark@psi.edu   303-980-0092
 (Corresponding Author)

[2]University of Arizona, Department of Planetary Sciences, Lunar & Planetary Laboratory 1629 E.
 University Blvd, Tucson, AZ 85721-0092, USA, rhb@lpl.arizona.edu

[3]Astrophysics Branch, NASA Ames Research Center, Moffett Field, CA 94035-1000, USA
 Dale.P.Cruikshank@nasa.gov

[4]U.S. Geological Survey, Mail Stop 964, Box 25046, Denver Federal Center, Denver, CO 80225, USA,
 gswayze@usgs.gov

Color not necessary for print version.

Highlights:
        Deuterium and carbon 13 are detected in the rings and on satellite surfaces in the Saturn system.
        New methods are presented for deriving isotopic ratios from reflectance spectra of solids.
        The D/H ratio of the water in Saturn's rings and icy satellites except Phoebe is close to
                terrestrial bulk Earth values.
        Phoebe's D/H is the highest value yet measured in the Solar system implying an origin in the
                cold outer Solar System beyond Saturn.
        Phoebe also has a high $^{13}C/^{12}C$ much greater than terrestrial, consistent with an origin in the cold
                outer Solar System.

Abstract

Isotopic ratios have long been used to learn about physical processes acting over a wide range of geological environments, and in constraining the origin and/or evolution of planetary bodies. We report the spectroscopic detection of deuterium in Saturn's rings and satellites, and use these measurements to determine the (D/H) ratios in their near-surface regions. Saturn's moons, Phoebe and Iapetus, show a strong signature of CO_2 and the ^{13}C component of this molecule is detected and quantified. Large averages of spectra obtained by the Cassini Visual and Infrared Mapping Spectrometer, VIMS, were computed for the rings and icy satellites. The observed intensities of the infrared absorptions in H_2O and CO_2 and their isotopes were calibrated using laboratory data and radiative transfer models to derive the D/H and $^{13}C/^{12}C$ ratios. We find that the D/H in Saturn's rings and satellites is close to the Vienna Standard Mean Ocean Water (VSMOW) and bulk Earth (4% lower than VSMOW) value except for Phoebe, which is 8.3 times the VSMOW value. This is the highest value for any Solar-System surface yet measured, and suggests that Phoebe formed from material with a different D/H ratio than the other satellites in the Saturn system. Phoebe's $^{13}C/^{12}C$ ratio is also unusual: 4.7 times greater than terrestrial, and greater than values measured for the interstellar medium and the galactic center. The high ^{13}C abundance in the CO_2 suggests that Phoebe was never warm enough for the large D/H ratio in its surface to have originated by evaporative fractionation of its water ice (e.g., from heating in the inner Solar System before its eventual capture by Saturn). We also report the detection of a probable O-D stretch absorption due to OD in minerals on Phoebe at 3.62 μm. This absorption is not detected on other Saturnian satellites. Stronger signatures of bound water absorptions are found in the dark material of Iapetus and we report a new detection of bound water at 1.9 μm. The position of this absorption matches that seen in spectra of hydrated iron oxides but does not match absorptions seen in spectra of tholins. Despite the strong bound water signature in the Iapetus dark material, no 3.62-μm OD absorption is seen in the spectra, further indicating the high deuterium level on Phoebe is unusual. As such, it is likely that Phoebe originated in a colder part of the outer Solar System, relative to the prevailing temperatures at Saturn's distance from the Sun.

Introduction

The origin of water on the Earth and throughout the Solar System and galaxy has been an area of continuous research, and determining isotopic ratios plays a key role in understanding the processes that have been operating since the Big Bang (Linsky *et al.*, 2006; Hallis, 2017; Weinberg, 2017). Current models of the deuterium to hydrogen isotopic ratio, D/H, are thought to indicate where each body formed in the Solar System, after accounting for geologic and atmospheric processing (Weinberg, 2017; Drake, 2005). Early in the formation of the Solar System, the proto-solar D/H is thought to have been about 0.25×10^{-4} corresponding to the observed values in Jupiter and Saturn, while the current interstellar medium (ISM) is on the order of 0.016×10^{-4}, lower today due to the destruction of deuterium by stars since the Big Bang (Robert, 2006). The inner Solar System, including Earth, Mars, Vesta, C- and S-type asteroids has a narrow range of D/H ratios, about 6 times higher than proto-solar, 1.5×10^{-4}. The D/H of the bulk Earth is $1.49(\pm 0.03) \times 10^{-4}$ (Lecuyer *et al.* 1998), while the oceans have been enhanced in D by about 4% to 1.56×10^{-4} for VSMOW. Outer Solar System comets have a range of D/H from the bulk Earth value and higher, though (Brown *et al.* 2012) documented sublimation cascades in laboratory studies that indicate the D/H ratio in cometary comae may not be representative of the bulk D/H ratio in the nucleus. Direct sensing of the surface ice that we report here avoids this problem.

Drake (2005) reviewed two possible origins for the water on the terrestrial planets 1) the inner Solar System accreted dry and water was delivered later, and 2) the inner Solar System accreted wet. If it accreted wet, the D/H is expected to change from the inner to outer Solar System due to the temperature gradient but some comets also have low D/H. Drake also noted the possibility that water in the terrestrial planets is a "late veneer" of asteroidal origin as discussed by Morbidelli *et al.* (2000). The "Grand Tack" model (Walsh *et al.* 2011) involves a migration of Jupiter inward then outward, scattering and mixing the S- and C-type asteroids, explaining the similar D/H observed in the inner Solar System. Lecluse et al. (1996) calculated that the ices that formed the core of Neptune have a D/H similar to VSMOW, but the D/H of proto-Uranian ices remain uncertain. The atmospheres of Uranus and Neptune are low compared to the bulk Earth D/H, but enriched with respect to the solar nebula. No model explains the observed higher than proto-solar D/H in the inner Solar System, the proto-solar Jupiter and Saturn values, higher Uranus and Neptune values, and diverse cometary values.

Recent studies indicate a dual origin for water in carbonaceous chondrites with one component lower than previously reported (Alexander *et al*, 2012; Stephant et al., 2017; Piani *et al.,* (2018). Piani et al., (2018) report a dominant deuterium-poor water component of D/H = 0.000101 ± 0.000006 in carbonaceous chondrites and suggest that this deteurium-poor water was a ubiquitous water reservoir in the inner proto-planetary disk. But Piani *et al.,* (2018) also found the least altered parts of the Paris CM chondrite to have D/H similar to VSMOW within the error bars. The higher bulk D/H in the meteorites is attributed to higher D in organics. Stephant *et al.* (2017) show the variation in D/H is large in chondrules in the Paris meteorite ranging from greater than to less than VSMOW. In reference to the primordial D/H ratio in the Paris meteorite, Stephant *et al.* states as an open issue "The hydrogen isotopic ratio of this source could be as low as ~0.0001, not that it conclusively is.

Yang *et al.* (2013) present a model for D/H in the solar nebula, with low D/H in the hotter inner disk, increasing to the cold outer disk, but then decreasing again in the outer regions, and predict water ice in the outer regions to have lower D/H on average. At the distance of Saturn, their model predicts D/H in the 0.0004 to 0.0008 range, some 2 to 5 times higher than we report in this paper for the rings and icy satellites (except Phoebe). Albertsson *et al.* (2014) also present models with D/H increasing from inner

to outer Solar System, with D/H at Saturn's distance ~0.003 to ~0.006, many times higher than reported here.

Alexander (2017) and Alexander *et al.*, (2018) reviewed the current understanding of the origin of water in the inner Solar System. The potential sources of volatiles for the Earth includes 2-4 wt% of CI/CM material to a volatile-depleted proto-Earth in order to explain the observed abundances of volatiles. He also concludes that isotopes of hydrogen are the most promising indicator to distinguish between models. Alexander states that models "should have become increasingly D-rich with distance from the Sun."

Measurement of D/H on icy satellites in the outer Solar System may shed light on the origin of water throughout the Solar System. Herein we show new measurements of D/H in Saturn's rings and satellites using reflectance spectroscopy, obtained using Cassini's VIMS instrument. Measuring deuterium abundances in ices on both very old and very young surfaces in the Saturn system allows constraints to be placed on the origin and evolution of these objects. In the case of Saturn's satellite Enceladus, the southern hemisphere is observed to be coated with deposits of water ejected by Enceladus' plumes from its interior. As such, the deuterium abundances in those deposits are likely representative of the bulk composition of Enceladus.

The NASA Cassini spacecraft orbited Saturn from 2004 to 2017. Tens of thousands of spectral image cubes of Saturn, its rings and its satellites were obtained by the Visual and Infrared Mapping Spectrometer, VIMS (Brown *et al.*, 2005). A recent recalibration has increased confidence in the validity of subtle spectral features (Clark *et al.*, 2018). Typical spectra of Saturn's satellites are illustrated in Figures 1a, 1b and 1c.

Laboratory Analysis of Deuterium in Ice

Laboratory spectra of natural and deuterium-doped H_2O ice are illustrated in Figures 2a, and 2b. Water ice in crystalline or amorphous form has orientational disorder, chiefly affecting the strength of its hydrogen bonds, resulting in very broad absorptions (Figure 2a). Pure D_2O or HDO ices show similarly-broad absorptions (Figure 2a). Deuterium in trace amounts tends to find the strongest hydrogen bonds in the crystal lattice via the mechanism of proton exchange, so its absorptions are not as broadened as those of H_2O (Figures 2a, 2b). The O-D stretch is located near 4.13 μm with a width of ~0.027 μm when deuterium is present in small abundances.

Observed band-depths in the laboratory reflectance spectra, relative to the 2-μm ice band depth are shown in Figure 2c. It is known that band strength in reflectance spectra varies with grain size and abundance of contaminants, so we measured laboratory spectra of natural H_2O and deuterium doped ice to calibrate the strength of the deuterium signature relative to the known deuterium abundance. It was found that the O-D absorption is slightly asymmetric, and in reflectance the band shifts from 4.132 to 4.137 μm as abundance decreases.

The equation that best fits this laboratory spectral trend is:

$$D/H = 1.9104*10^{-06} + 0.0030167x + 0.0067252x^2 + 0.00081011x^3, \qquad \text{(eqn 1)}$$

where x = OD band depth / 2-μm band depth. This ratio approximately compensates for variations in band depth due to changes in grain size.

Radiative transfer models were run by adjusting grain size distribution to match the ice band depths of the laboratory data as well as the reflectance levels, and specifically fitting the 3.6-4.5-μm region using the optical constants of Mastrapa *et al*. (2008, 2009). An absorber was added over the 4.13-μm OD stretch envelope to match the strength of the OD feature. The derived absorption coefficient was scaled to the strength for 100% deuterium (idealized pure D_2O without broadening from orientational disorder). The OD stretch absorption coefficient idealized to 100% OD was found to be 80,000 cm^{-1}. The OD stretch absorption coefficient is shown with the absorption coefficients for H_2O ice in Figure 3. An absorption coefficient of ~ 80,000 cm^{-1} for the O-D stretch compared to about 560 cm^{-1} in H_2O ice at 4.13 μm, enables the detection of deuterium at levels less than that in Vienna Standard Mean Ocean Water (VSMOW), given sufficient signal-to-noise ratio, S/N.

The laboratory mixtures made for this study were constructed at room temperature with liquids. The resulting samples would have a small percentage of molecules that exist in the D_2O state. At temperatures where proton exchange can happen on short (lab) timescales, and the mixture is in equilibrium (i.e., what you would expect if you started with liquid and then froze it), the system should go to 1:2:1 H_2O:HDO:D_2O. For example, if one started with 3% D_2O, as in Figure 2a, for every 200 water molecules, 6 of which started out as D_2O, the rest as H_2O, the six D_2O molecules will interact with six H_2O molecules, and the deuterons will distribute themselves in the mix with a ratio 3(H_2O):6(HDO):3(D_2O) forming the 12 molecules (because there are twice as many ways to make a mixed molecule versus a homogeneous molecule). The mixture would have 191 molecules as H_2O (188 + 3), 6 molecules as HDO and 3 molecules as D_2O at any instant.

In crystalline ice, the O-H stretch near 3-μm shows a broad envelope with a strong peak absorption flanked on each side by slightly less strong absorptions (Figure 3). The complexity is in part due to symmetric and asymmetric stretching modes in the ice crystal. One might expect to see two or more O-D stretching modes, however, only one is observed in spectra of ice containing small amounts of deuterium (Figure 2b and 3). Therefore, the single observed absorption near 4.13 μm represents the trace levels of deuterium in the ice. The observed band asymmetry and shifting of the band position may be due to vibrational coupling and/or differing contributions from symmetric and asymmetric stretches and/or different proportions of HDO versus D_2O in the sample.

Radiative transfer models, following the methodology of Clark *et al*. (2012), including contaminants and ice grain size distributions, and including spectral effects of sub-micrometer grains, which are common in the Saturn system, were computed for a wide variety of conditions. Sample spectra are shown in Figures 4a and 4b. Similar radiative transfer models were run to match spectral features in Saturn's rings and satellites. Calculated band depths in models versus those of observed spectra were used to calculate the D/H ratio.

A second method, which shows good agreement with radiative transfer models, uses a simple band depth ratio: the OD band depth divided by the 2-μm H_2O combination band depth. Band depths change in reflectance as a function of grain size and contaminant as illustrated in Figures 4a and 4b. Band depths versus grain size are shown in Figure 5a.

The modeled OD versus 2-μm H_2O band-depth ratio is shown in Figure 5b. For relatively clean ice, which includes the ice in Saturn's rings, the cleaner ice on the icy satellites, and for the mean grain diameters observed, 1-100 micrometers, the band-depth-ratio is relatively stable and can be used to determine the D/H. The modeled results agree with lab data (Figure 2c). The curves in Figure 5b represent greater extremes than those observed on the rings and icy satellites, except Phoebe, where

only radiative transfer models were used because the abundances of the contaminants are too large to allow the use of the clean-ice-band-depth-ratio method.

For clean ice and the band-depth-ratio model, we estimate the D/H ratio to be accurate to 15 to 20% when the mean ice grain size is in the few- to ~100-micrometer diameter range. As contamination increases, a multi-component radiative transfer model like that described in Clark *et al*. (2012) is required to derive accurate D/H ratios. Results of experiments, using clean ice, show agreement within about 15% between radiative transfer models and the band-depth-ratio method (examples in Table 1).

O-D Stretch in Spectra of Saturn's Rings and Satellites

To achieve maximum precision in our D/H determinations, we constructed large averages of spectra of icy surfaces in the Saturn system, including the B-ring, Enceladus' northern and southern hemispheres, Rhea (global), Hyperion (global), Iapetus icy regions, and Phoebe (global). The observed O-D absorption depths are typically 2-4%, much higher than residual calibration and formal errors in the VIMS data (Figures 6, 7, 8). An example continuum-removed measurement is illustrated in Figure 7 for Saturn's B-ring.   Error bars are the standard deviation of the mean after bad-pixel rejection from RC19 calibrated data using the VIMS team pipeline (Clark *et al*., 2018)

Measured band depths and derived D/H values are given in Table 1 along with values for other objects reported in the literature.

The O-D stretch is observed in VIMS spectra of Saturn's rings and satellites with sufficient signal-to-noise ratio (S/N). To confirm that the 4.13-µm absorption is real and not a result of a calibration error, we studied the spectrum of Saturn's F-ring obtained at high phase angles, where the main signal is from diffracted light, not light transmitted through grains (Figure 8), and where, the apparent O-D stretch feature would also appear if it were a calibration artifact. We observe no residual O-D absorption greater than 0.1% band depth in the high-phase, F-ring spectrum, establishing with high confidence that the 4.13-µm absorptions in the rings and satellites can be measured with sufficient precision to determine the D/H.

Carbon Dioxide and the $^{13}C/^{12}C$

Saturn's satellites also show signatures of CO_2 (Buratti *et al.*, 2005; Clark *et al.*, 2005, 2008, 2012; Cruikshank *et al*., 2010; Pinilla-Alonso *et al*., 2011). The absorptions are strong enough to allow detection of ^{13}C on Phoebe and Iapetus (Figure 9), and in turn to determine the spectroscopic band-strength ratio of ^{12}C to ^{13}C in CO_2. We derive the ratio of the equivalent widths of the ^{13}C and ^{12}C absorptions to be 0.053±0.006 on Phoebe, 0.012±0.0012 on Iapetus, and 0.010±0.001 for the laboratory spectrum. These ratios are related to the $^{13}C/^{12}C$ ratio, but there may be effects due to intra-molecular and inter-molecular coupling that will contribute to systematic errors in the isotopic abundances derived using equivalent-width measurements that need to be quantified, but are believed to be small. For comparison, the terrestrial value of the $^{13}C/^{12}C$ ratio is 0.011, and vibrational coupling may explain the 10% higher high lab mixture result (note the error bar in our lab measurement overlaps with the terrestrial value). The local interstellar medium is 0.014±0.0033 (Boogert, 2000). In any case, Iapetus' $^{13}C/^{12}C$ appears close to terrestrial, but Phoebe is anomalous, having higher than expected ^{13}C.

In the terrestrial environment, $^{13}C/^{12}C$ ranges from about 0.0115 to 0.0096 (Coplen *et al*., 2002), much lower than observed on Phoebe. Biologic activity on Earth depletes ^{13}C and burning fossil fuels is

causing long term reduction in ^{13}C in Earth's atmosphere. The main carbon reservoirs on Earth are sedimentary organic matter, the biosphere, and sedimentary carbonates and they differ in their isotopic compositions due to differing fractionation mechanisms (Coplen *et al.*, 2002 and references therein) but no mechanism on Earth produces the high ^{13}C seen on Phoebe.

Because the CO_2 bands arising from Phoebe's and Iapetus' dark material have different central wavelengths, and because the ^{13}C absorption strengths are so different, their surface evolutions are likely to have been different. The different band positions and isotopic band strengths on Iapetus argues for a different source for the CO_2 rather than from Phoebe. Thus, while Phoebe dust coats the leading side of Iapetus, if there were any CO_2 in the Phoebe dust on ejection from Phoebe, it is apparently lost on its way from Phoebe to Iapetus.

The band positions of CO_2 on Saturn's satellites have been previously reported (Clark *et al.* 2005, 2008, 2012) and studied in detail by Cruikshank *et al.* (2010). CO_2 band positions are observed to vary in position in terrestrial minerals (Figure 10). The CO_2 in the Saturn system generally correlates with the dark material on satellite surfaces, but in the case of Iapetus it is found in all regions observed in the September 10, 2007 flyby, including some parts of the higher albedo region and the transition zone between the dark material and the brighter icy surface. There are statistically significant differences in the central wavelength of CO_2 across the range of surfaces on Iapetus (Pinilla-Alonso *et al.* 2011), but always shifted toward shorter wavelengths than the band on Phoebe. The band is strongest in the Iapetus low albedo regions, suggesting that it may be preferentially trapped at a molecular level in the dark material.

The molecular configuration of CO_2 in H_2O ice or on a granular surface of the low-albedo material, which is presumed to be refractory, is uncertain, and may differ from one satellite to the next. In all cases, except Phoebe, the CO_2 band is shifted to shorter wavelengths and can be attributed to some complexing of CO_2 with the host material, either confined to a cage of H_2O molecules as a clathrate (e.g., Blake *et al.* 1991), or in a looser configuration (e.g., Chaban *et al.* 2007); in all cases the band is shifted to shorter wavelengths (Cruikshank *et al.* 2010). In the case of Iapetus, pure CO_2 ice is unstable against sublimation, and it may be produced on the surface by photolysis of oxygen and carbon (Palmer and Brown, 2011), and in the course of synthesis it may enter into a complexed configuration with H_2O or with refractory grains of a different composition. While the band position needs further study, the ^{12}C and ^{13}C absorptions are readily apparent in VIMS data, enabling the ratio to be derived, as shown in this work.

Deuterium in Minerals

As illustrated in Figure 1c, an absorption band is detected in spectra of Phoebe at 3.62 μm. The absorption feature is not seen in spectra of any other Saturn satellite or rings in the VIMS spectra we have analyzed. We have surveyed possible origins of the absorption and can rule out organics and other compounds because they display strong absorption bands at other wavelengths that are not observed in spectra of Phoebe. Organics are detected in spectra of Phoebe and Iapetus (Clark *et al.* 2005, 2012, Dalle Ore *et al.* 2012, Cruikshank *et al.* 2014) but the C-H stretching fundamentals are weak, meaning any combination band at 3.62 μm would be even weaker, ruling out an organic origin. The 3.62-μm absorption band appears consistent with OD in minerals. OD is commonly seen in terrestrial minerals (e.g. Figures 11, 12) and the band position changes significantly from mineral to mineral.

Clark *et al*. (2012) concluded that the 3-μm absorption in spectra of the dark materials on Phoebe and Iapetus (see Figure 1c) was at a unique position matched only by hydrated iron oxides (e.g. in hematite). Could the deuterium responsible for the 3.62-μm absorption in spectra of Phoebe be in the hydrated iron oxides? The VIMS RC19 calibration enables further insight into this question. We extracted Iapetus dark material spectra, producing a 49-pixel average (Figure 1c) which shows a 1.9-μm, bound-water absorption with little confusion from water ice. The 1.9-μm absorption also shows a good fit to the hydrated iron oxide spectrum (Figure 13), in agreement with the stronger spectral identification of hydrated iron oxides in the 3-μm absorption in the spectra of the dark material on Iapetus. We detect no 3.62-μm OD absorption in the Iapetus spectra. This implies that the minerals on Phoebe either have a higher deuterium content, or the 3.62-μm absorption has a different origin. In either case, this comparision points to differences in the surface composition of Phoebe versus Iapetus even though the two surface compositions have much in common, including Phoebe dust coating the surfaces of both satellites. Laboratory experiments need to be conducted with deuterated hydrated iron oxides to see if a 3.62 μm OD stretch is present.

Laboratory work combined with radiative transfer modeling is required to calibrate O-D stretch absorptions in minerals to provide a means of determining deuterium abundance. That, unfortunately, is beyond the scope of this paper.

Fractionation scenarios by heating within the Solar System

The measured D/H ratios for Saturn's rings and satellites are compared with other Solar System objects, the proto-solar nebula and galactic entities in Figure 14 and Table 1. Saturn's rings and satellites, except Phoebe, have D/H similar to carbonaceous chondrites (CC) meteorites, bulk Earth and terrestrial ocean water. Phoebe's high deuterium value is anomalous. In fact, it is even higher than that of the Martian atmosphere which has experienced significant fractionation due to atmospheric escape (Owen *et al*., 1988). Could Phoebe have been similarly processed?

<u>**Scenario 1: Phoebe was formed elsewhere and later captured by Saturn**</u>.

A way to account for the large D/H ratio of Phoebe is to hypothesize that Phoebe formed from a reservoir of materials with a similar D/H ratio as that of the Saturn system, but in an independent orbit around the Sun. Proto-Phoebe subsequently underwent heavy, evaporative fractionation increasing the surface D/H ratios to what we observe today. Phoebe was then captured by Saturn. Though possible, such a scenario is implausible. If an evaporative process were responsible for the observed D/H ratios, and if the material that formed this "proto-Phoebe" had D/H ratios that were roughly terrestrial, Phoebe would have had to have lost most of its volatile material. Even using a simple, Rayleigh fractionation model for such a large fractionation event (Figure 15), which provides a strong upper limit to how much evaporative isotopic fractionation could occur on a proto-Phoebe's surface, 99+% of Phobe's original volatile component would have had to have evaporated to produce the observed D/H ratios. A Rayleigh-fractionation model assumes D and H are well mixed in the remaining material, which is not possible in a moon-sized, solid object without highly unrealistic assumptions about diffusive vapor transport in porous media. Thus, the model in Figure 15 represents a very strong upper limit to the D/H ratio that could be attained during evaporative fractionation. In a real icy moon, the downward diffusive transport, and thus the final D/H ratio would be much lower (Brown *et al*., 2012; Moores *et al*., 2012; Lecuyer *et al*., 2017). Such a huge fractionation having occurred by evaporation, either by a

liquid-water or an icy, proto Phoebe is highly unlikely without the object having lost virtually all of its volatile material. Thus, if Phoebe's original D/H ratio were similar to that of the other icy objects in the Saturn system, and were subsequently increased by evaporative fractionation to what we see today, Phoebe's physical appearance, along with its bulk and chemical properties should be that of an object composed almost entirely of rock and organics. That, however, is not what is observed, and we hypothesize that Phoebe must have formed elsewhere with a higher D/H source of water and was later captured by Saturn.

Scenario 2: Phoebe was formed within the Saturn system and then suffered a large isotopic-fractionation event during or after formation that did not operate on most of the other bodies in the Saturn system.

Such a scenario could be imagined if Phoebe formed in the coolest regions of the proto-Saturn system, and subsequently migrated closer to the proto-planet, suffering a large amount of evaporation of its initial ice fraction, presumably from heat radiated by a proto-Saturn that was much hotter than the present day object. Phoebe was then moved by gravitational interactions from a presumably regular orbit close to Saturn, to the eccentric, distant orbit we see today. Unfortunately, such a scenario has a similar flaw as does that of Scenario 1 above: If Phoebe were heated enough to have driven off all but a few percent of its icy material so as to accomplish the necessary D/H fractionation, it would have a very different appearance and set of physical and chemical properties from that of the Phoebe we know.

With D/H at 7.6 ± 1.7 times that of the average of the other icy bodies in the Saturn system (Table 1), it is quite clear that the D/H of Phoebe is very different. An obvious implication of that is either Phoebe did not form from a reservoir of material with a D/H ratio similar to that of most of the other objects in the Saturn system, including the planet, or if it did, then the D/H ratio of Phoebe's surface material must have been strongly altered during or after its formation. There are several general processes that could drive isotopic fractionation under Solar System conditions, including evaporative/condensative, chemical and photolytic. Chemical and photolytic processes typically produce far lower isotopic fractions than observed for Phoebe (Brown *et al.*, 2012), but evaporative/condensative processes can be effective at driving large fractionations within the expected range of formation temperatures for icy Solar-System objects (Brown *et al.*, 2012; Jura, 1982; Messenger and Walker, 1997; Keller *et al.*,2000). An obvious question is: what scenarios could explain Phoebe's surface D/H ratio when compared to the other icy surfaces in the Saturn system?

Discussion

There likely are many possible ways to account for Phoebe's large D/H ratio relative to the rest of the Saturn system, but there are only a few that are plausible. One plausible scenario calls for Phoebe to form in a region of the Solar System well beyond the orbital distance of Saturn, where the constituent material condensed from the pre-solar nebula at much lower temperatures. It is well known that materials in molecular clouds, most prominently interstellar grains, have strongly enhanced deuterium abundances relative to terrestrial abundances, driven primarily by isotopic fractionation of simple molecular species such as CH_4, NH_3, H_2O and other simple molecules having hydrogen as a component (Jura, 1982; Messenger and Walker, 1997; Keller *et al.*, 2000). Many processes can drive that fractionation, such as ion-molecule reactions and condensation onto interstellar grains, producing D/H ratios high enough to account for the large D/H ratio seen on Phoebe's surface (Tielens *et al.*, 2010; Roberts *et al.*, 2003; Roberts *et al.*, 2004). Similarly, such processes could also explain the $^{13}C/^{12}C$

enhancement seen on Phoebe's surface. Phoebe's appearance, surface composition, density and geological state suggest that Phoebe is an object with a bulk composition dominated by water ice, with a surface layer of mostly pure water ice, which, based on the depth of many impact craters on its surface, is several to several tens of km thick (Clark *et al.*, 2005; Porco *et al.*, 2005). In this scenario, Phoebe formed from a reservoir of material that included abundant water ice with a D/H ratio similar to what we observe. It was then captured at some later time by Saturn, where it has been in orbit ever since, but preserves a surface that is chemically and isotopically similar to its primordial state. This view is consistent with the conclusion of Johnson and Lunine (2005) that Phoebe's composition is significantly different from Saturn's regular satellites, supporting the contention that it formed in the region of the solar nebula where Pluto and Triton condensed and was subsequently captured by Saturn.

We considered fractionation scenarios for Phoebe by postulating heating events occurring elsewhere within the Solar System, and/or within the Saturn system in an event that did not otherwise affect other bodies in the Saturn system. We have argued that such scenarios require Phoebe to have lost all but a few percent of its water and other volatiles, for which there is no geologic evidence. Furthermore, because CO_2 is quite volatile at temperatures where water ice readily evaporates in a vacuum, the high abundance of CO_2 seen in Phoebe's spectrum also argues against extensive heating and evaporation of Phoebe's volatile components.

Conclusions

We have presented laboratory data and radiative transfer model calculations to calibrate the strength of trace deuterium in H_2O ice and presented methods for deriving the D/H ratio from reflectance spectra of solid water. We showed that the D-O stretch is readily detected in reflectance spectra of Saturn's icy satellites and rings. We also showed the detection of ^{13}C in CO_2 and derive the ^{13}C to ^{12}C ratio. We found that the rings and icy satellites except Phoebe have D/H similar to bulk terrestrial levels. Both D/H and $^{13}C/^{12}C$ are very high on Phoebe. The only other satellite with high enough CO_2 to determine $^{13}C/^{12}C$ is Iapetus and we found it was also similar to terrestrial values, leaving Phoebe as the only object measured in the study to stand out as significantly different.

The most plausible way for Phoebe to have the high observed D abundance is for it to have formed from material that had a high D abundance relative to that of the bulk of the material from which the rest of the Saturn system formed. Otherwise, for Phoebe to have formed out of material with a D abundance similar to that of the rest of the Saturn system, and then to have its surface D abundance dramatically enhanced by evaporative fractionation, requires Phoebe to have present-day characteristics similar to objects that are composed primarily of rock and organics, which is not what we observe. Thus, Phoebe's high D abundance is likely a consequence of Phoebe having formed outside the Saturn system, probably in the distant outer Solar System and subsequently captured by Saturn.

An interpretation of the origin of terrestrial water from current data is that it was brought to Earth by carbonaceous chondrites (Morbidelli *et al.* 2000; see review by Alexander *et al.*, 2018) and the ocean water was enriched in D by hydrolysis of D-rich organic compounds. If the water depleted (D/H ~0.0001, proto-Earth) in the clays of CI/CM chondrites is combined D-rich organic matter to give a bulk chondrite D/H similar to VSMOW, it is hard to argue other scenarios from comets to Saturn's rings and satellites, all coincidentally resulting in VSMOW values for the D/H. Indeed, Marty et al. (2016) argued that comets like 67P could have delivered some volatiles to the Earth without changing bulk D/H significantly. Comets like Hartley 2 with terrestrial D/H could also be a source of water. It is apparent from the data in Table 1 and Figure 14 that a number of icy bodies, from comets to Saturn's

rings and satellites, have essentially bulk terrestrial D/H, and not lower. The terrestrial-like D/H of Saturn's rings and satellites may indicate a similar water source for the inner and outer Solar System, or at least a change in models where the D/H varies less from inner to outer Solar System, less than a factor of two from Earth to Saturn.

The high D/H (~1%) in interstellar clouds, diverse D/H values in comets, and the high Phoebe results, may be showing that there is a large variation in the D/H among distant cold objects. The existence of the high D/H on Phoebe appears to indicate a mechanism that could bring high D/H ices from the outer Solar System to the inner system (Saturn inward).   D/H measurements on the icy satellites of Jupiter, Uranus, and Neptune are needed to show the larger trends in the Solar System, but such measurements can only be done above the Earth's atmosphere.

Acknowledgments

References

Albertsson T.. Semenov, D., Henning Th., *2014.* Chemodynamical Deuterium Fractionation in the Early Solar Nebula: the Origin of Water on Earth and in Asteroids and Comets. *Astrophys. J.*, **784**:39, 1-11.

Alexander, C.M.O.D., Bowden, R., Fogel, M. L., Howard, K. T., Herd, C. D. K., Nittler.*L. R., 2012.* The Provenances of Asteroids, and Their Contributions to the Volatile Inventories of the Terrestrial Planets. *Science* **337**, 721–723.

Alexander, CMOD, 2017. The origin of inner Solar System water, *Phil. Trans. Royal Soc. A.* **375**, doi: 10.1098/rsta.2015.0384.

Alexander, CMOD, K. D. McKeegan, and K. Altwegg, 2018. Water Reservoirs in Small Planetary Bodies: Meteorites, Asteroids, and Comets, *Space Sci Rev* **214**, 36. https://doi.org/10.1007/s11214-018-0474-9

Blake, D., Allamandola, L., Sandford, S, Hudgins, D., Freund, F., 1991. Clathrate hydrate formation in amorphous cometary ice analogs in vacuo. *Science* **254**, 548-551.

Boogert, A. C. A., 2000. ISO-SWS observations of interstellar solid $^{13}CO_2$: heated ice and the Galactic $^{12}C/^{13}C$ abundance ratio. *Astron. Astrophys.* **353**, 349-362.

Brown, R.H., Baines, K.H., Bellucci, J.P., Bibring, B.J., Buratti, E., Bussoletti, F., Capaccioni, P., Cerroni, P., Clark, R.N., Coradini, D.P., Cruikshank, P., Drossart, Y., Formisano, R., Jaumann, Y., Langevin, D.J., Matson, T.R., 2005. The Cassini visual and infrared mapping spectrometer investigation. *Space Science Rev.,***115 (1-4)**, 111-168.

Brown, R. H., Lauretta, D. S., Schmidt, B., & Moores, J., 2012. Experimental and theoretical simulations of ice sublimation with implications for the chemical, isotopic, and physical evolution of

icy objects. *Planetary and Space Science,* **60**(1)*,* 166-180. DOI: 10.1016/j.pss.2011.07.023

Buratti, B. J., Cruikshank, D. P., Brown, R. H., Clark, R. N., Bauer, J. M., Jaumann, R., McCord, T. B., Simonelli, D. P., Hibbitts, C. A., Hansen, G. B., Owen, T. C., Baines, K. H., Bellucci, G., Bibring, J.-P., Capaccioni, F., Cerroni, P., Coradini,A., Drossart, P., Formisano, V., Langevin, Y., Matson, D. L., Mennella, V., Nelson, R. M., Nicholson, P. D., Sicardy, B., Sotin, C., Roush, T. L., Soderlund, K., and Muradyan, A., 2005. Cassini Visual and Infrared Mapping Spectrometer Observations of Iapetus: Detection of CO_2. *Astrophy. J.* **622**, L149-L152

Chaban, G. M., Bernstein, M., and Cruikshank, D. P. 2007. Carbon dioxide on planetary bodies: Theoretical and experimental studies of molecular complexes. *Icarus* **187**, 592-599.

Clark, R.N., Brown, R. H., Jaumann, R., Cruikshank, D. P., Nelson, R. M., Buratti, B. J., McCord, T. B., Lunine, J., Baines, K. H., Bellucci, G.,Bibring, J.-P., Capaccioni, F., Cerroni, P., Coradini, A., Formisano, V., Langevin, Y., Matson, D. L., Mennella, V., Nicholson, P. D., Sicardy, B., Sotin, C., Hoefen, T. M., Curchin, J. M., Hansen, G., Hibbits, K., and Matz K.-D., 2005. Compositional maps of Saturn's moon Phoebe from imaging spectroscopy. *Nature,* **435**, 66-69. doi:10.1038/nature03558.

Clark, R.N., Swayze, G.A., Wise, R., Livo, E., Hoefen, T., Kokaly, R., Sutley, S.J., 2007. USGS digital spectral library splib06a. *U.S. Geological Survey*, Data Series 231, http://speclab.cr.usgs.gov/spectral-lib.html

Clark, R.N., Brown, R.H., Jaumann, R., Cruikshank, D.P., Buratti, B., Baines, K.H., Nelson, R.M., Nicholson, P.D., Moore, J.M., Curchin, J., Hoefen, T., and Stephan, K., 2008. Compositional mapping of Saturn's satellite Dione with Cassini VIMS and implications of dark material in the Saturn system. *Icarus* **193**, p 372-386, doi:10.1016/j.icarus.2007.08.035.

Clark, R. N., Cruikshank, D. P., Jaumann, R., Brown, R. H., Stephan, K., Dalle Ore, C. M., Livo, K. E., Pearson, N., Curchin, J. M., Hoefen, T. M., Buratti, B. J., Filacchione, G., Baines, K. H., and Nicholson P. D., 2012. The Composition of Iapetus: Mapping Results from Cassini VIMS. *Icarus* **218**, 831-860.

Clark, R. N., Brown, R. H., Lytle, D. M., and Hedman, M., 2018. The VIMS Wavelength and Radiometric Calibration 19, Final Report. *NASA Planetary Data System, The Planetary Atmospheres Node*, 30p. http://atmos.nmsu.edu/data_and_services/atmospheres_data/Cassini/vims.html

Coplen, T. B., Hopple, J. A., Böhlke, J. K., Peiser, H. S., Rieder, S. E., Krouse, H. R., Rosman, K. J. R., Ding, T., Vocke, R. D. Jr., Révész, K. M., Lamberty, A., Taylor, P. and De Bièvre, P., 2002. Compilation of Minimum and Maximum Isotope Ratios of Selected Elements in Naturally Occurring Terrestrial Materials and Reagents. *U.S. Geological Survey*, Water-Resources Investigations Report 01-4222.

Cruikshank, D. P., Meyer, A. W., Brown, R. H., Clark, R. N., Jaumann, R., Stephan, K., Hibbitts, C. A., Sandford, S. A., Mastrapa, R. M. E., Filacchione, G., Dalle Ore, C. M., Nicholson, P. D., Buratti, B. J., McCord, T. B., Nelson, R. M., Dalton, J. B., Baines, K. H., and Matson, D. L., 2010. Carbon dioxide on the satellites of Saturn: Results from the Cassini VIMS investigation and revisions to the VIMS wavelength scale. *Icarus* **206**, 561-572, doi:10.1016/j.icarus.2009.07.012

Cruikshank, D. P., Dalle Ore, C. M., Clark, R. N., Pendleton, Y. J., 2014. Aromatic and aliphatic organic materials on Iapetus: Analysis of Cassini VIMS data. *Icarus* **233**, 306-315.

Dalle Ore, C. M., Cruikshank, D. P., Clark, R. N. 2012. Infrared spectroscopic characterization of the low-albedo materials on Iapetus. *Icarus* **221**, 735-743.

Drake, M. J., 2005. Origin of water in the terrestrial planets. *Meteoritics & Planetary Science* **40**, 519–527.

Fanale, F.P. and Salvail, J.R., 1984. An idealized short-period comet model - Surface insolation, H_2O flux, dust flux, and mantle evolution. *Icarus* **60**, 476-511.

Fanale, F.P. and Salvail, J.R., 1987. The influence of CO ice on the activity and near-surface differentiation of comet nuclei. *Icarus* **84**. 403-413.

Gonfiantini, R., 1978. Standards for stable isotope measurements in natural compounds: *Nature*, **271**, 534–536.

Hallis, L. J., 2017. D/H ratios of the inner Solar System. *Phil. Trans. R. Soc*. **A 375**: 20150390. http://dx.doi.org/10.1098/rsta.2015.0390

Johnson, T. V., Lunine, J. I., 2005. Saturn's moon Phoebe as a captured body from the outer Solar System. *Nature* **435**, 69-71.

Jura, M. 1982. Abundance fluctuations in the interstellar medium. in *Advances in Ultraviolet Astronomy*, Y. Kondo, J. M. Mead, and R. D. Chapman, eds, NASA CP-2238, 54-60.

Kedziora-Chudczer, L., Bailey, J., Horner, J., 2013. Observations of the D/H ratio in methane in the atmosphere of Saturn's moon, Titan-where did the Saturnian system form? *Proceedings 12th Australian Space Science Conference*, 53-64. https://arxiv.org/pdf/1302.4503.pdf

Keller, L.P., Messenger, S., Bradley, J.P., 2000. Analysis of a deuterium-rich interplanetary dust particle and implications for presolar materials in IDPs. *J. Geophys. Res.* **105**, 10397-10402.

Linsky, J.L., Draine, B. T., Moos, H. W., Jenkins, E. B., Wood, B. E., Oliveira, C., Blair, W. P., Friedman, S. D., Gry, C., Knauth, D., Kruk, J. W., Lacour, S., Lehner, N., Redfield, S., Shull, J. M., Sonneborn, G., and Williger, G. M., 2006. What is the total deuterium abundance in the local galactic disk? *Astroph. J*. **647**, 1106-1124.

Lecluse, C., Robert, F., Gautier, D., Guiraud, M., 1996. Deuterium enrichment in giant planets. *Planetary & Space Sci.* **44**, 1579-1592.

Lecuyer, C., Gillet, P., Robert, F., 1998. The hydrogen isotope composition of seawater and the globalwater cycle, *Chemical Geology* , **145**, 249-261.

Lecuyer, C., Royer, A., Fourel, F., Seris, M., Simon, L.,Robert, F. 2017. D/H fractionation during the sublimation of water ice. *Icarus*, **285**, 1-7.Marty, B., Altwegg, K., Balsiger, H., Bar-Nun, A, Bekaert, D.V., Berthelier, J.-J., Bieler, A., Briois, C., Calmonte, U., Combi, M., De Keyser, J., Fiethe, B., Fuselier, S.A., Gasc, S., Gombosi, T.I., Hansen, K.C., Hässig, M., Jäckel, A., Kopp, E., Korth, A., Le Roy, L., Mall, U., Mousis, O., Owen, T., Rème, H., Rubin, M., Sémon, T., Tzou, C.-Y.., Waite, J.H.,

Wurz, P., 2017. Xenon isotopes in 67P/Churyumov-Gerasimenko show that comets contributed to Earth's atmosphere. *Science* **356**, 1069-1072.Mastrapa, R.M., Bernstein, M.P., Sandford, S.A., Roush, T.L., Cruikshank, D.P., Dalle Ore, C.M., 2008. Optical constants of amorphous and crystalline H_2O–ice in the near infrared from 1.1 to 2.6 μm. *Icarus* **197**, 307–320.

Mastrapa, R.M., Sandford, S.A., Roush, T.L., Cruikshank, D.P., and Dalle Ore, C.M., 2009. Optical constants of amorphous and crystalline H_2O-ice: 2.5–22 μm (4000–455 cm^{-1}). *Astroph. J.* **710**, 1347–1356.

Messenger, S., and Walker, R.M., 1997. Evidence for molecular cloud material in meteorites and interplanetary dust. in *Astrophysical Implications of the Laboratory Study of Presolar Materials*, ed. T.J. Bernatowitcz & E. Zinner, *AIP Conf. Proc.*, **402**, 545-564.

Moores, J.E., Brown, R.H., Lauretta, D.S., Smith, P.H., 2012. Experimental and theoretical simulation of sublimating dusty water ice with implications for D/H ratios of water ice on Comets and Mars. *Planetary Science* **1**, 2-28.

Morbidelli, A., Chambers, J., Lunine, J.I., Petit, J.M., Robert, F., Valsecchi, and G.B.., Cyr, K.E., 2000. Source regions and time scales for the delivery of water to Earth, *Meteoritics & Planetary Science*, **35**, 1309-1320.

Owen, T., Maillard, J. P., de Bergh, C., Lutz, B. L., 1988. Deuterium on Mars: The Abundance of HDO and the Value of D/H. *Science*, **240**, 1767.

Palmer, E. E., Brown, R. H., 2011. Production and detection of carbon dioxide on Iapetus. *Icarus* **212**, 807-818.

Piani, L., Robert, F., Remusat, L., 2015. Micron-scale D/H heterogeneity in chondrite matrices: A signature of the pristine solar system water? *Earth Planet. Sci. Lett.* **415**, 154-164.

Piani, L.,Yurimoto, H., Remusat, L., 2018. A dual origin for water in carbonaceous asteroids revealed by CM chondrites. *Nature Astronomy* **2**, 317-323.

Pinilla-Alonso, N., Roush, T. L., Marzo, G. A., Cruikshank, D. P., Dalle Ore, C. M., 2011. Iapetus surface variability revealed from statistical clustering of a VIMS mosaic: The distribution of CO_2. *Icarus* **215**, 75-82

Porco,C.C., Baker, E., Barbara, J., Beurle, K., Brahic, A., Burns, J. A., Charnoz, S., Cooper, N., Dawson, D. D., Del Genio, A. D., Denk, T., Dones, L., Dyudina, U., Evans, M. W., Giese, B., Grazier, K., Helfenstein, P., Ingersoll, A. P., Jacobson, R. A., Johnson, T. V., McEwen, A., Murray, C. D., Neukum, G., Owen, W. M., Perry, J., Roatsch, T., Spitale, J., Squyres, S., Thomas, P. C., Tiscareno, M., Turtle, E., Vasavada, A. R., Veverka, J., Wagner, R., West, R., 2005. Cassini Imaging Science: Initial Results on Phoebe and Iapetus. *Science* **307**, 1237-1242.

Robert, F., 2006. Solar System Deuterium/Hydrogen Ratio. in *Meteorites and the Early Solar System II,* Dante Lauretta and Harold Y. McSween, eds, University of Arizona Press, 341-351.

Roberts, H., Herbst, E., Millar, T.J., 2003. Enhanced deuterium fractionation in dense interstellar cores resulting from multiply deuterated H_3^+. *Astroph. J. Let.* **591** (1), L41-L44.

Roberts, H., Herbst, E., Millar, T.J., 2004. The chemistry of multiply deuterated species in cold, dense interstellar cores. *Astronomy & Astrophysics* **424**, 905-917.

Stephant, A., Remusat, L., Robert, F., 2017. Water in type I chondrules of Paris CM chondrite. *Geochim. Cosmochim. Acta* **199**, 75-90.

Tielens, A.G.G.M. 2010. The Physics and Chemistry of the Interstellar Medium. *Cambridge U. Press*. 510 pp. 2nd edition.

Waite Jr, J. H., Lewis, W. S., Magee, B. A., Lunine, J. I., McKinnon, W. B., Glein, C. R., Mousis, O., Young, D. T., Brockwell, T., Westlake, J., Nguyen, M. J., Teolis, B. D., Niemann, H. B., McNutt Jr, R. L., Perry, M., and Ip, W. H., 2009. Liquid water on Enceladus from observations of ammonia and ^{40}Ar in the plume. *Nature* **460,** 487-490.

Walsh K.J., Morbidelli A., Raymond S.N., O'Brien D.P., Mandell A.M., 2011. A low mass for Mars from Jupiter's early gas-driven migration. *Nature* **475**, 206-209.

Weinberg, D.H., 2017. On the Deuterium-to-hydrogen Ratio of the Interstellar Medium. *Astrophys. J.*, **851**.

Yang, L., Ciesla, F.J., Alexander, C. M. O'D., 2013. The D/H ratio of water in the solar nebula during its formation and evolution. *Icarus* **226**, 256-267.

```
                                    Table 1
                      Deuterium
Object                -------------------------------
                      O-D Stretch  position   width   2-micron  O-D /     D/H
                      band depth   (microns)  (micron) Band depth 2-um OH                    ID          Comment

H2O ground 90K        0.030 ±0.003 4.137      0.026    0.841     0.036  0.00012 ±0.00001     spd0432 r5116  H2O ground 90K MCTA IR ext av8 REFL
H2O +0.0005 D2O       0.122 ±0.002 4.135      0.0278   0.812     0.150  0.00061 ±0.00001     spd0432 r5041  H2O + 0.0005 D2O vol 80K av13 REFL
h20 +0.0025 D2O       0.341 ±0.005 4.132      0.0340   0.814     0.419  0.00250 ±0.00002     spd0432 r5054  h20 + 0.0025vol D2O=HDO 80K av8 REFL

         D/H = 1.9104E-06 + 0.0030167x + 0.0067252x^2 + 0.00081011x^3,  x = OD/2-micron band depth ratio

Ring B                0.0352±0.004 4.138      0.039    0.780     0.045  0.00016 ±0.00003     spv0029 r1772  b-ring 640msS01-45RC19inccor 21882pwV950
                                                                                                           RT model D/H: mdl4f= 0.000161, mdl2t1= 0.000173
                                                                                                           OD/2-um ratio D/H   = 0.00015

Enceladus NorthHem    0.0416±0.008 4.146      0.044    0.660     0.063  0.00022 ±0.00006     spv0042 r299   enceladus_s08-12rc19 irN 80+160ms 5229pixels
Enceladus SouthHem    0.0372±0.008 4.147      0.022    0.669     0.056  0.00019 ±0.00006     spv0042 r303   enceladus_s08-12rc19 irS 80+160ms 12273pixels
Enceladus Plume INMS                                                   0.00029 +0.00015                   Waite et al, 2009
                                                                              -0.00007

Rhea                  0.0352±0.004 4.135      0.035    0.681     0.052  0.00018 ±0.00003     spv0040 r 271  rhea_2004-52RC19-640m sigav 10628/con ed
                                                                                                           Model comparison to B-ring, lab1, lab2

Titan atmosphere                                                        0.000143±0.000016                  Kedziora-Chudczer et al., 2013

hyperion              0.031 ±0.006 4.129      0.047    0.555     0.056  0.00020 ±0.00006     spv0042 r 310  hyperion r15rc19-640ms a1203 VIMS RC19
hyperion              0.037 ±0.006 4.129      0.047    0.574     0.064  0.00023 ±0.00006     spv0042 r 312  hyperion r15rc19-640ms brt av198 VIMS

Iapetus icy           0.0364±0.005 4.143      0.036    0.727     0.050  0.00017 ±0.00003     spv0042 r 308  iapetus r49rc19-640ms brt av1904 VIMS

phoebe                0.0186±0.004 4.142      0.035    0.176      *   0.0013  ±0.0003         spv0029 r1684  phoebe RC19VIMS global average 3143pixels
                                                                                                           RT models mdl15t9+0.0015D, mdl15t9+0.0010D
                                                                                          * surface too dark for valid D/H using the band ratio method.

Saturn Icy average of best spectra: Ring B + Rhea + Iapetus icy D/H = (0.00016 + 0.00018 + 0.00017)/3 = 0.00017 ±0.000020

f-ring diffractuion  0.002 ±0 0.002 (reflectance = 0.09 at 4.2 microns)   -            spv0029 r1390  f-ring hiphcalcmp rev 195
                                                                                                      Illustrates maximum residual calibration error

Callisto NIMS         0.008 ±0.006 4.123      0.014    0.055     0.145  0.0006 ±0.0005      spd0453 r 517  wav515 Callisto I/F Carlson 10/2004 ch=326 326

VSMOW                                                                  0.00015576 ±0.0000001          Gonfiantini, 1978
Bulk Earth                                                             0.000146                       Lecuyer et al., 1998
Six CM Chondrite D-poor                                                0.000101 ±0.000006             Piana et al, 2018
Paris CM Chondrite least altered                                       0.000145 ±0.000025             Piana et al, 2018
Vesta                                                                  0.000131 to 0.000150           Alexander, 2017 + references

galactic disk withing 1 kpc of the sun:                               0.0000231                      Linsky et al, 2008

Terrestrial Water                                                      0.00007866 to 0.0001759        Coplen et al., 2002
Terrestrial Silicates Ca 2 NaH(SiO 3 ) (pectolite)                    0.00008894 to 0.0001120        Coplen et al., 2002
Terrestrial Aluminum and iron hydroxides,                             0.0001215  to 0.0001545        Coplen et al., 2002
Terrestrial organics                                                  0.00007305 to 0.0001537        Coplen et al., 2002
Terrestrial Atmosphere                                                0.00013458 to 0.0001838        Coplen et al., 2002

Mars, young rocks                                                     ~0.0008 to 0.001                Hallis, 2017
Mars, old rocks                                                       ~0.0002 to 0.0005               Hallis, 2017
```
VSMOW = Vienna Standard Mean Ocean Water
Comments:

REFL = reflectance measurement. MCTA = FTIR detector used in the laboratory measurements,
av8, av13 = number of FTIR spectra averaged (8, 13). ext = external chamber (cold) used. 90K = temperature in Kelvin
S numbers, like S01 – S45 are Cassini sequence numbers. 1-45 is approximately the first half of the mission.
640 ms = 640 millisecond integration per VIMS pixel. Incor = inclination correction (solar incidence correction roreflectance).
B-ring: 21882pwV950 = 21882 pixels, 640 milliseconds each averaged. V950 = code for the wavelengths.
Rhea: sigav 10628/con = 10628 pixel averages using a sigma clipped average to reject spikes. /con = continuum removed.
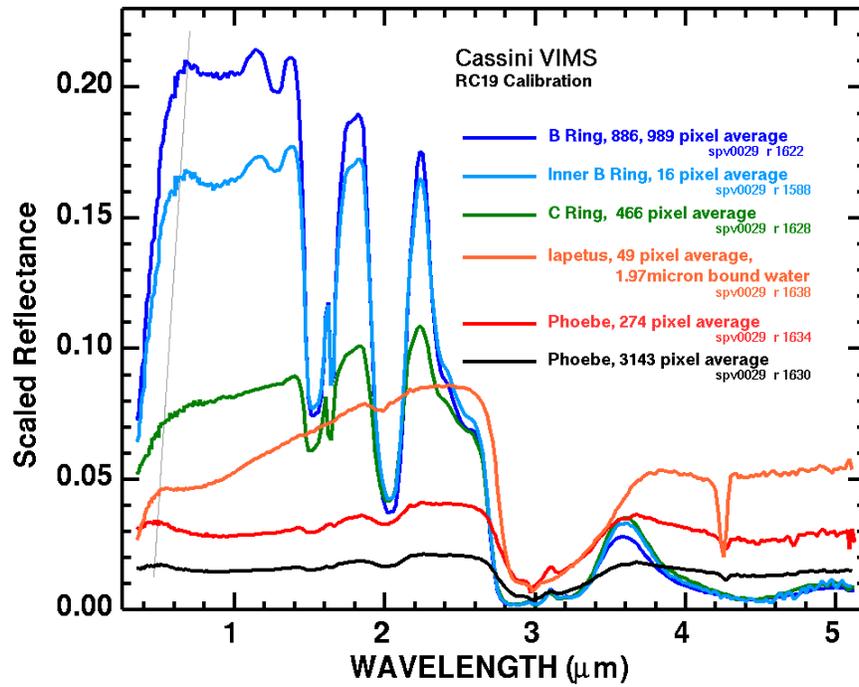
Figure 1a. Example spectra showing the diversity of spectral signatures in the Saturn system. The sp* entries (e.g., spv0029 r1622) are the unique identification codes to each spectrum. Spectra are calibrated using the VIMS team pipeline with the final team calibration, RC19 (Clark *et al.*, 2018).
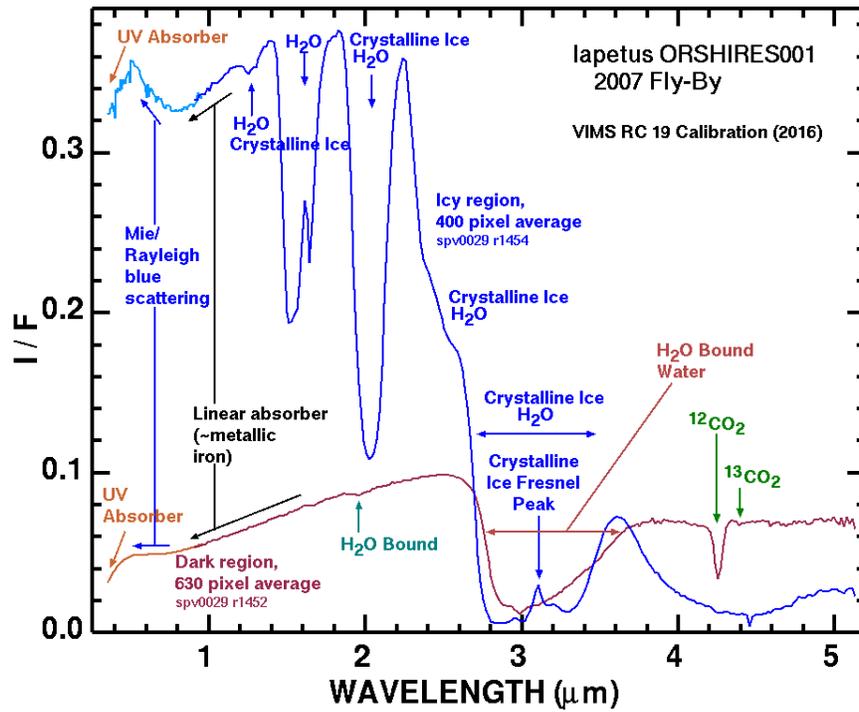
Figure 1b. Spectral properties of different regions on Iapetus. The rings and Saturnian satellites, except for Titan, show similar ice spectral properties.
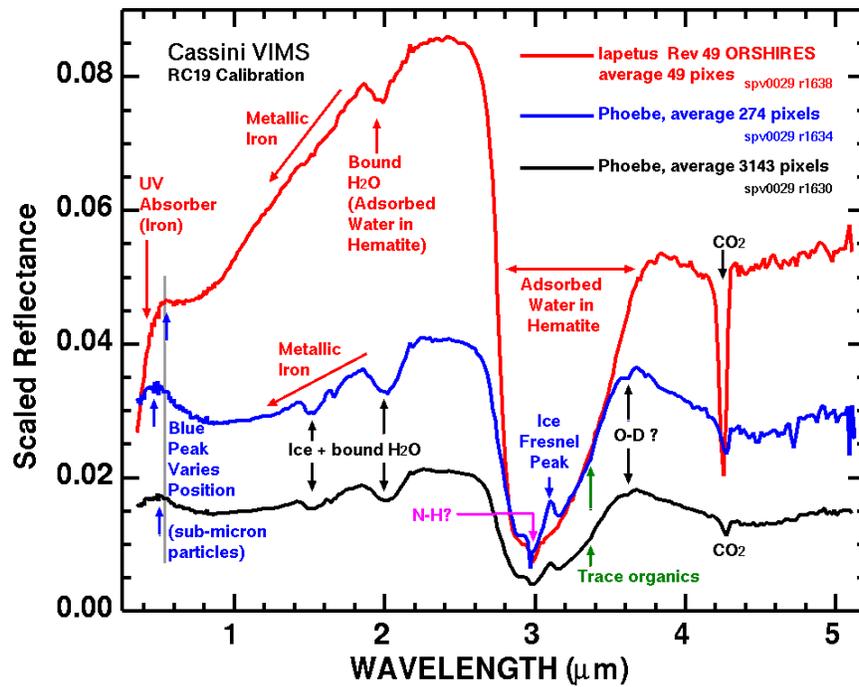
Figure 1c. Spectral properties of Phoebe and the dark region on Iapetus. Identifications of spectral features follows Clark *et al.*, 2012. The presence of an ammonia absorption, N-H, is uncertain because the VIMS instrument has an order sorting filter gap at this location. The O-D stretch at 3.62 μm in the Phoebe spectra is reported here for the first time, as is the ~1.96-μm, bound-water absorption in the Iapetus spectrum. The gray line near 0.55 μm is to better show the shifting position of the blue peak position.
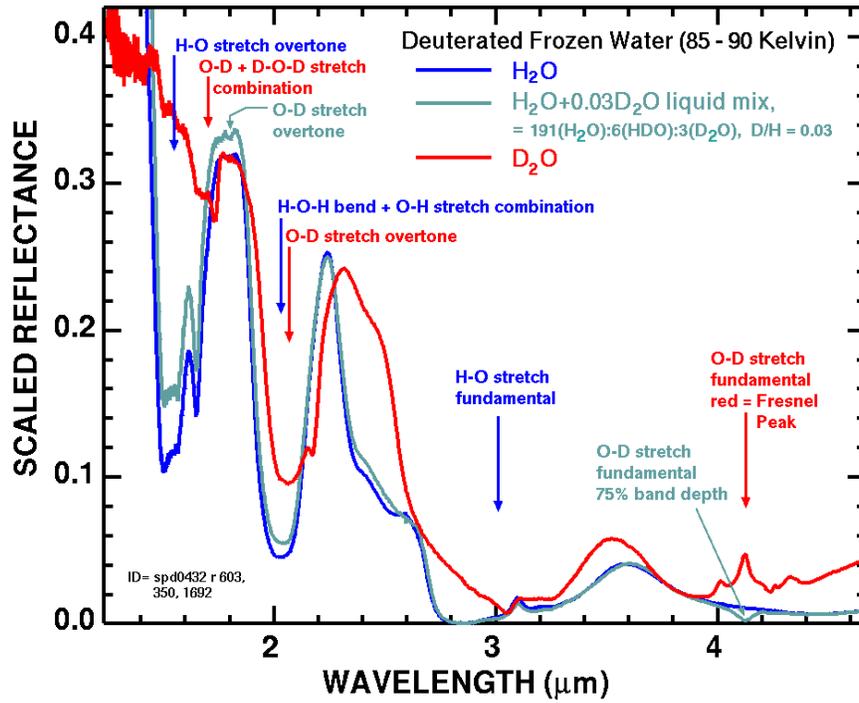
Figure 2a. Laboratory spectra of fresh water H_2O ice, D_2O ice, and ice with added deuterium.
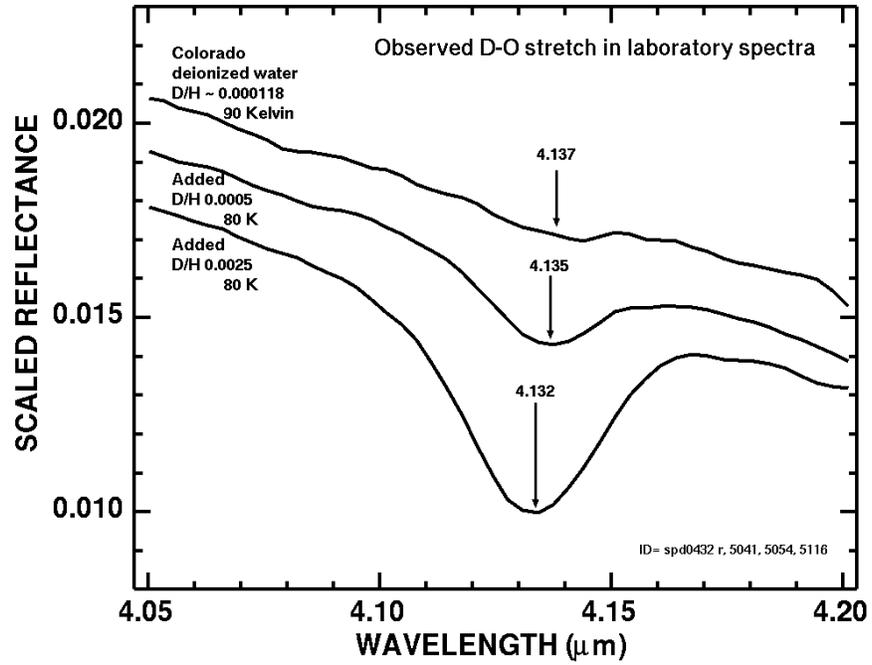
Figure 2b. Lab spectra of the O-D stretch with different deuterium abundances made by addition of D_2O to deionized H_2O water (bottom two spectra). The absorption band shift may be due to changes in vibrational coupling as the deuterium abundance increases.
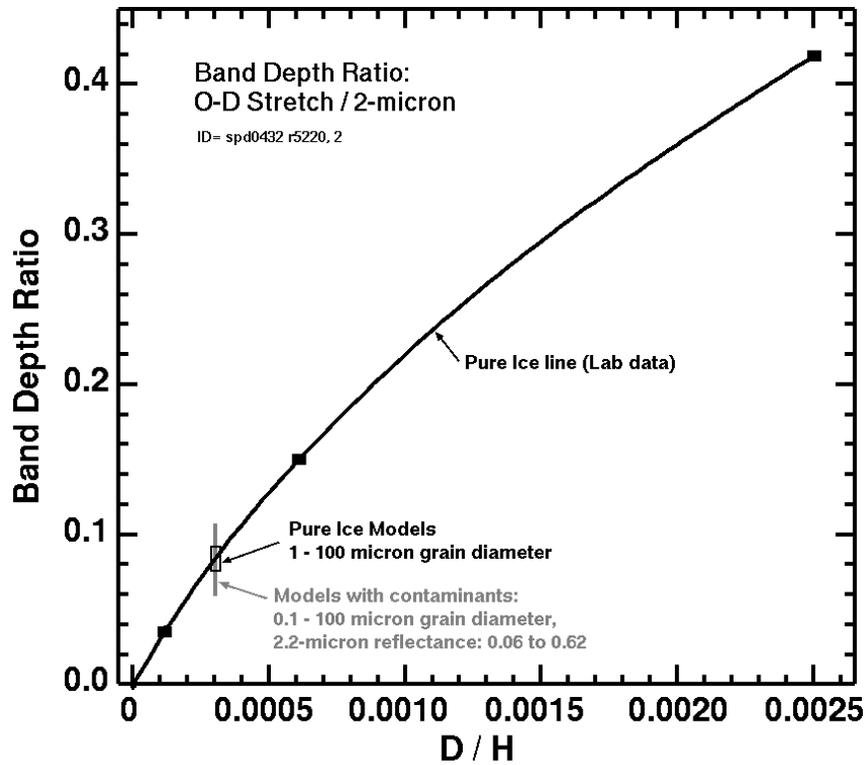
Figure 2c. Measured band-depth ratio of the 4.13-μm O-D stretch to the 2-μm H_2O combination absorption band derived from laboratory spectra of ice with added deuterium (solid squares). The data from models (open box and vertical line) cover a larger range of spectral properties than observed in spectra of the rings and icy regions of Saturn's satellites. See text and Figures 4a and 4b.
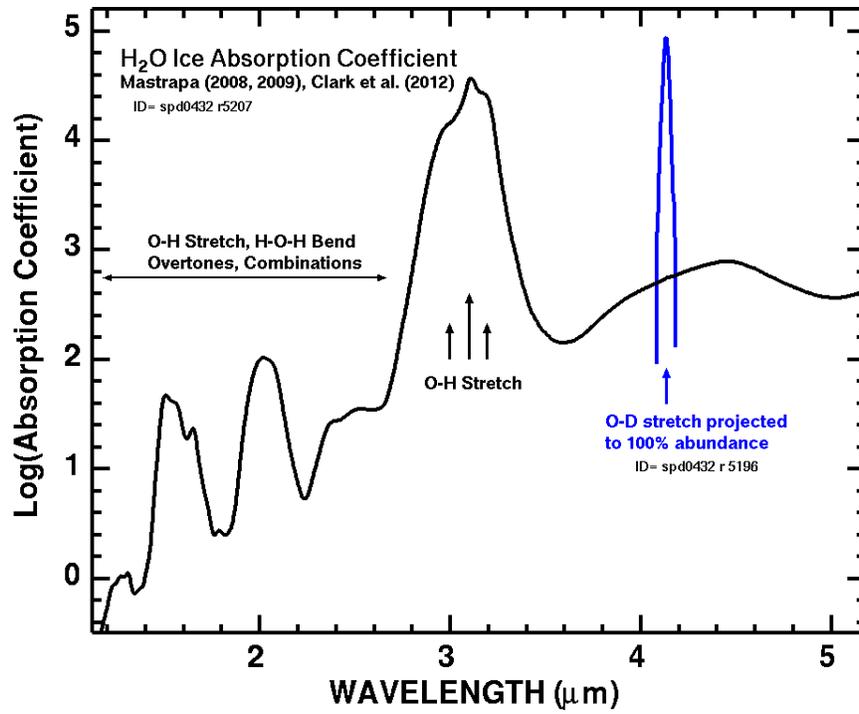
Figure 3. Derived O-D stretch absorption coefficient projected to 100% D₂O compared to the absorption coefficients for pure H₂O.
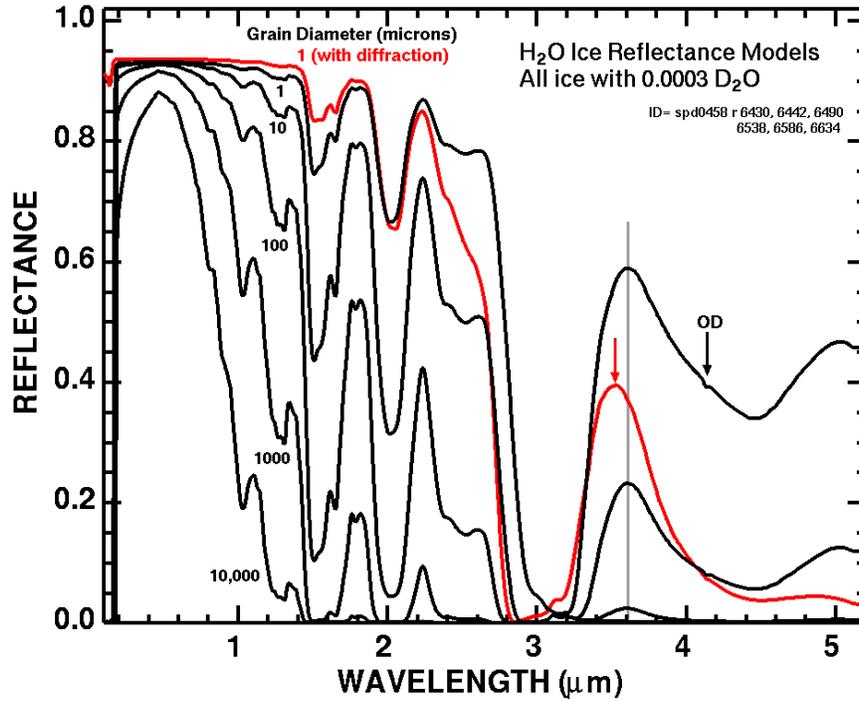
Figure 4a. Radiative transfer models of H_2O with D/H = 0.0003. The added diffraction from small particles (red line), using the model from Clark *et al.* (2012) illustrates the changes in band shape, and position, as well as the 3.6-μm peak position (gray line versus red arrow), but minimally affects the 4.13-μm O-D absorption depth divided by the 2-μm absorption depth (see text and Figures 4b, 5a).
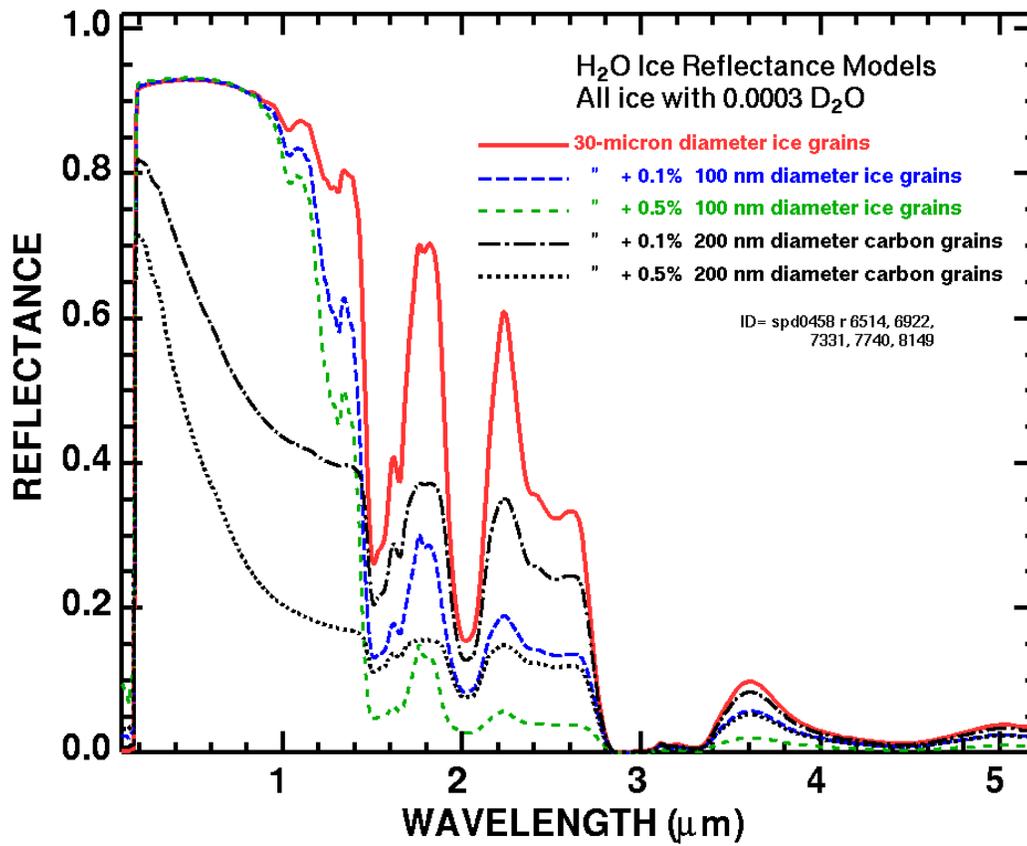
Figure 4b. Radiative transfer models of H_2O with D/H = 0.0003 and mixed with sub-micrometer ice or carbon grains.
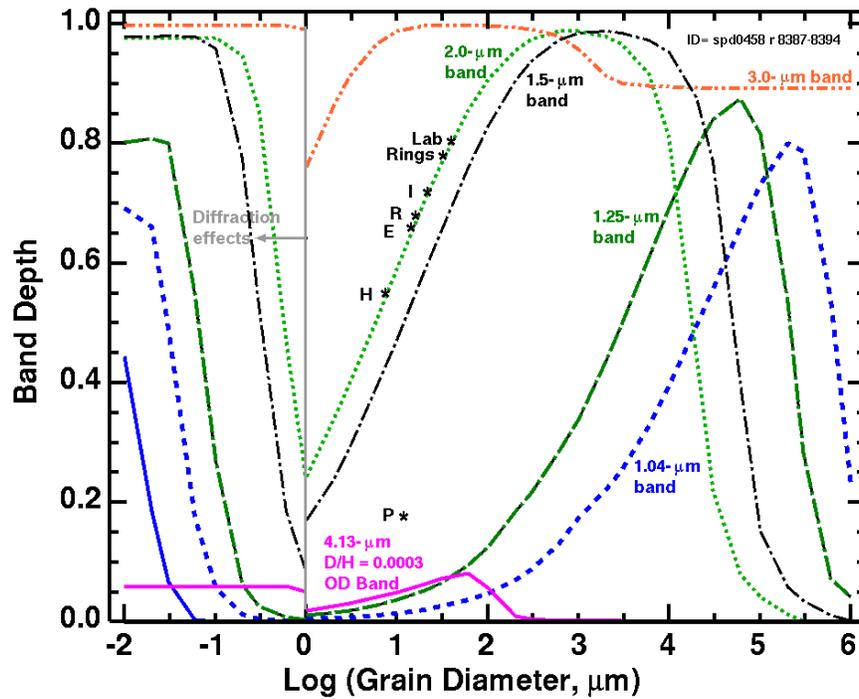
Figure 5a. Band depth model versus grain diameter. Diffraction is turned on for particle diameters less than 1 μm. The observed band depths for the 2-μm absorption are indicated by the letters H, E, R, I, and P, where H = Hyperion, E = Enceladus, R= Rhea, I = Iapetus, and P = Phoebe. Phoebe does not fit on the trend lines because of the high abundance of dark contaminants on Phoebe's surface.
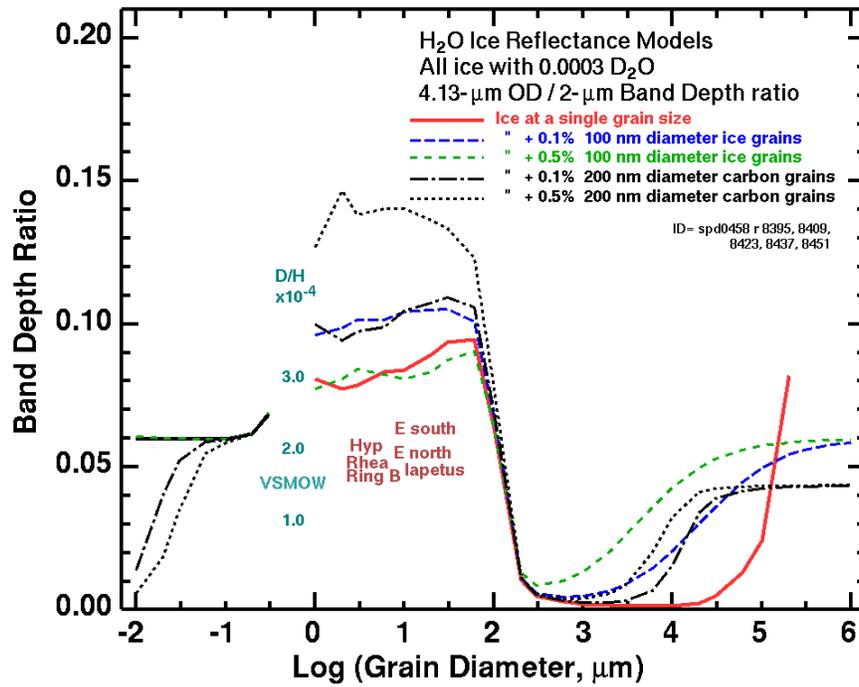
Figure 5b. Band depth ratios for different ice grain sizes and contaminants. The D/H scale is for clean ice. E south = Enceladus' southern hemisphere. E north = Enceladus' northern hemisphere.
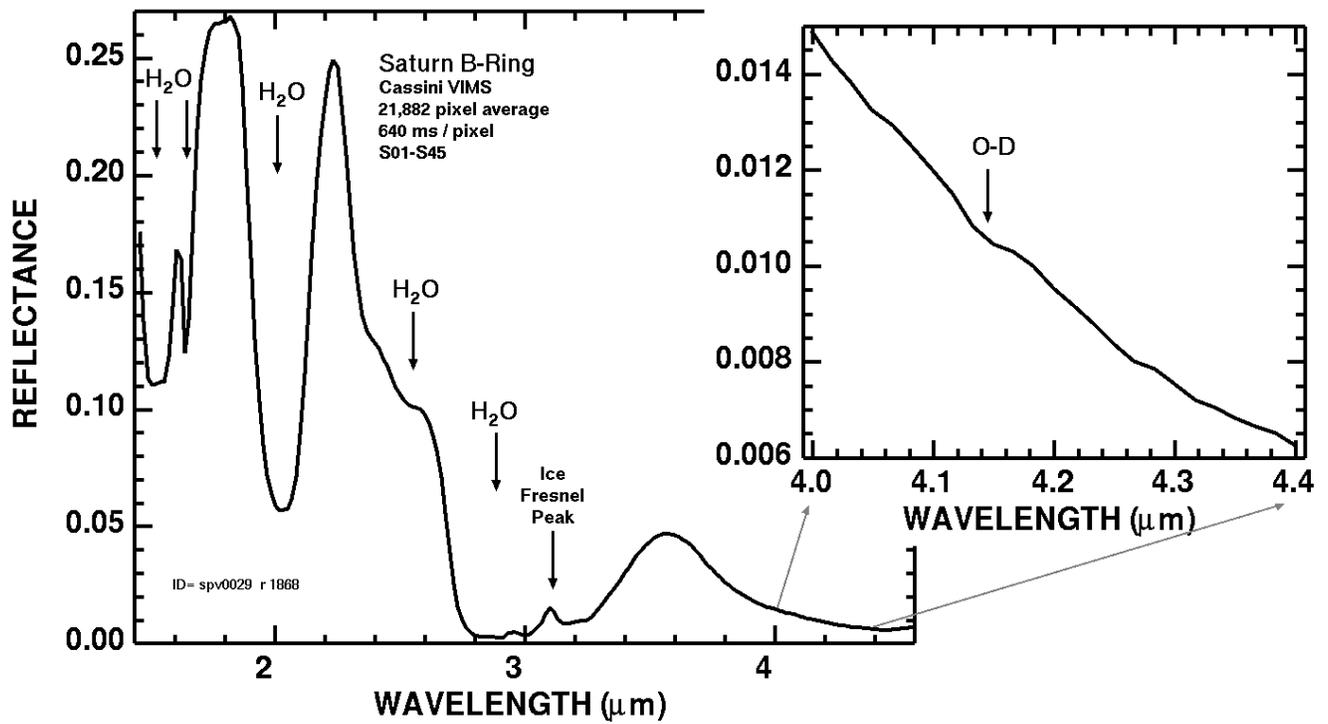
Figure 6. VIMS spectrum of Saturn's B-ring. Note the O-D band at 4.13 μm is too small to see at the scale of the full plot but is seen in the inset. The error bars are smaller than the line width.
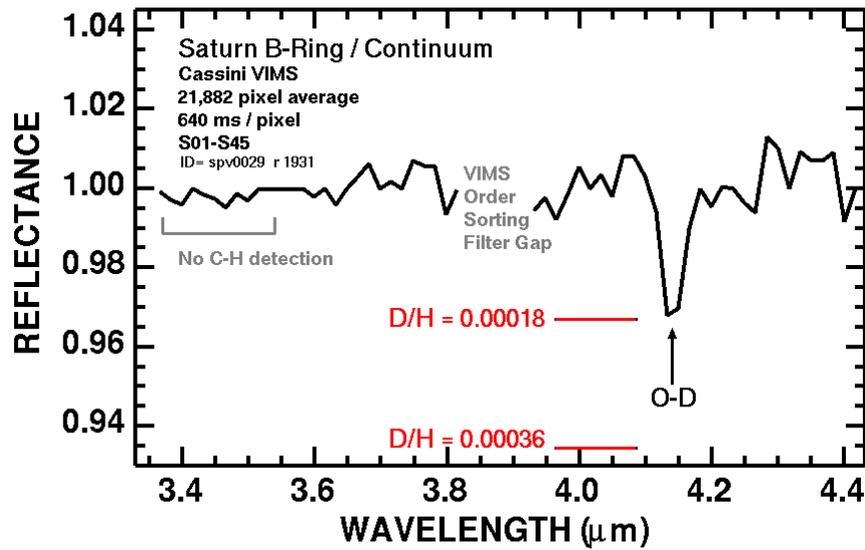
Figure 7. O-D stretch in spectra of the Ring B showing strong signal above residual noise. The error bars are smaller than the line width. The residual spectral structure, at the ~0.5% level, may be due to trace contaminants, or residual calibration differences (see Clark *et al,* 2018). Improvement of the calibration needs further study and is beyond the scope of this paper. In any case, the O-D absorption strength is clearly above remaining noise and calibration uncertainties. The D/H levels were derived from radiative transfer models fitting the 1- to 5-μm spectrum, including observed band depths and continuum levels.
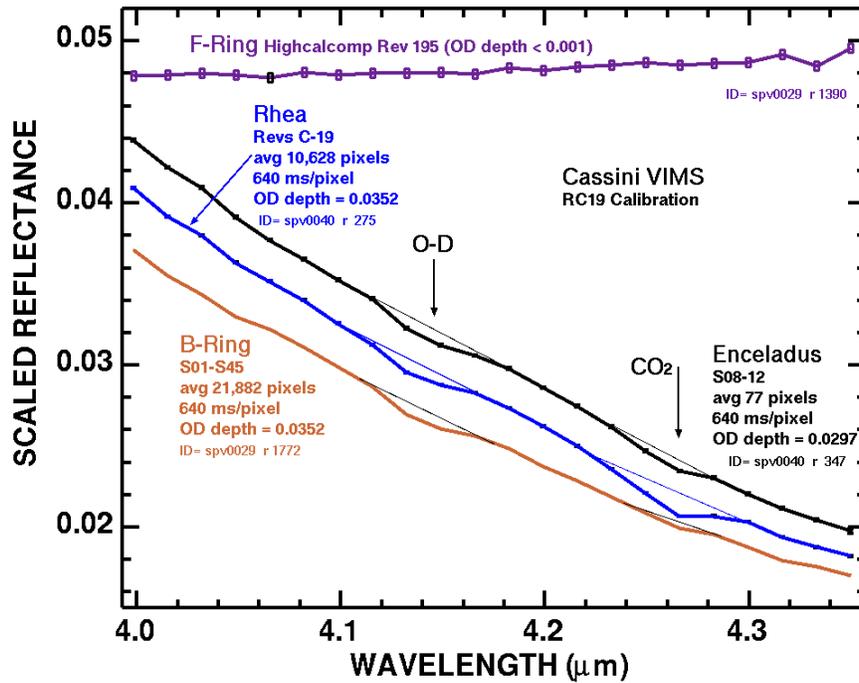
Figure 8. Enlarged O-D spectral region showing the O-D and CO_2 absorptions. At this scale, error bars are smaller than the line widths. The F-ring spectrum was made at high phase angle and so the signal is mainly due to diffraction and no OD or CO_2 should be present. Indeed, there is no OD feature in the F-ring spectrum greater than 0.1%.
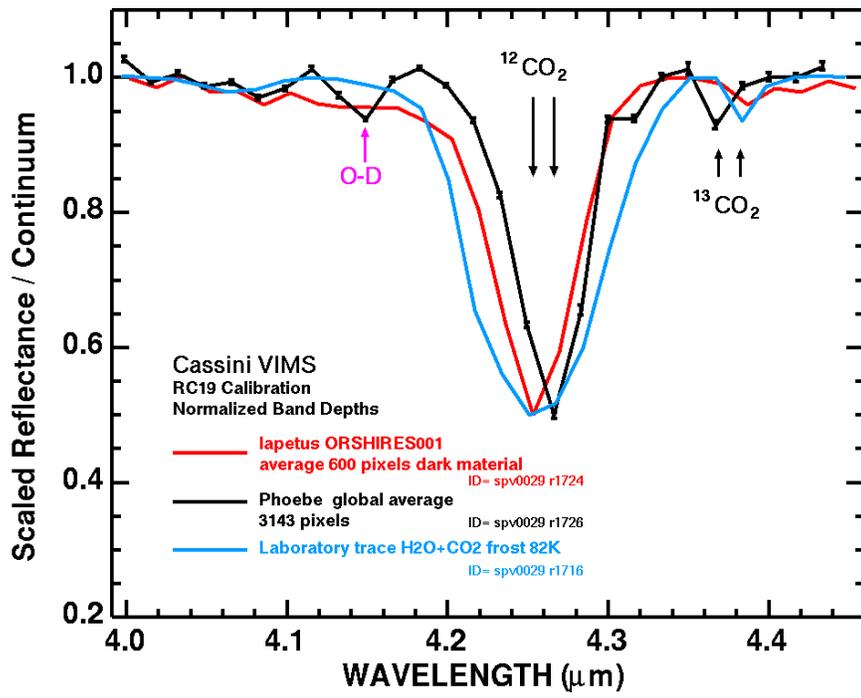
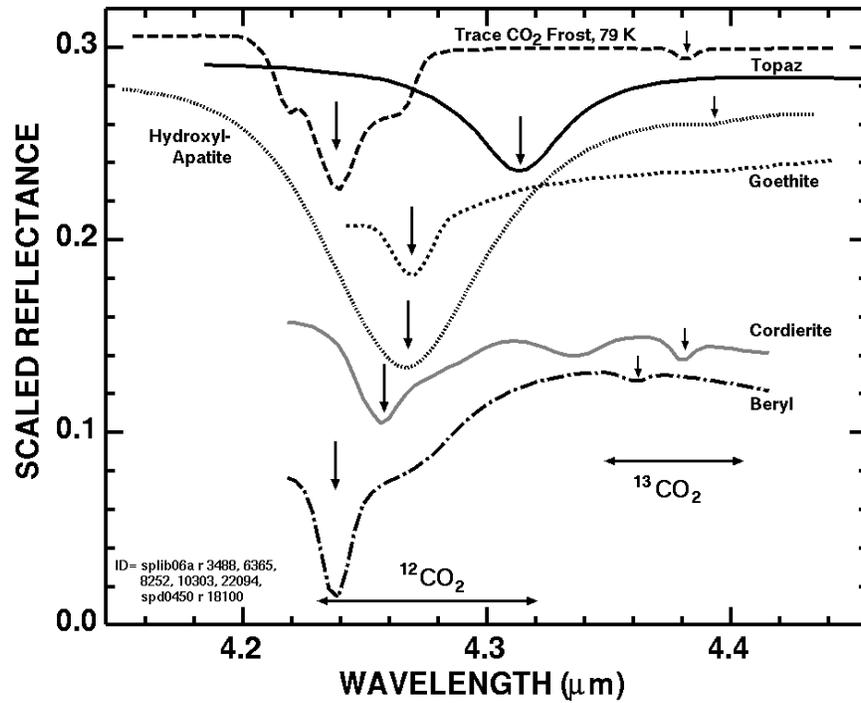Figure 9. The O-D and carbon isotope absorptions in spectra of Phoebe and Iapetus, are compared to that of a laboratory spectrum of H_2O and CO_2 frost.

Figure 10. Observed CO_2 trapped in terrestrial minerals shows wide variations in wavelength position, shape and width. Positions and widths vary similarly in spectra of Saturn system surfaces. Data from USGS spectral library 06 (Clark *et al.*, 2007). The CO_2 frost is from this study.
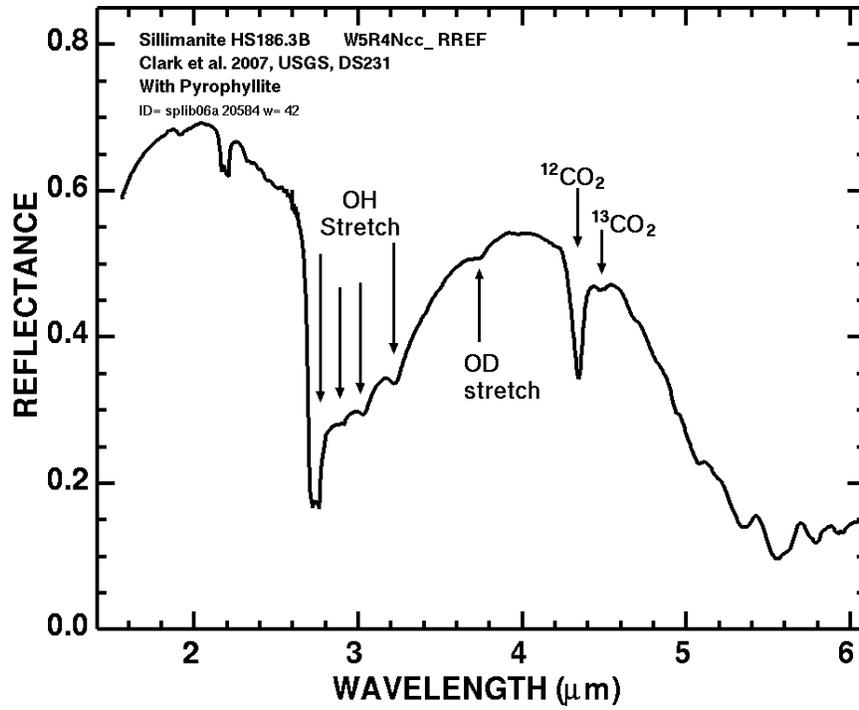
Figure 11. Illustration of an O-D stretch in a spectrum of a terrestrial mineral, also carbon 12 and 13 in CO_2. Data from USGS spectral library 06 (Clark *et al*., 2007).
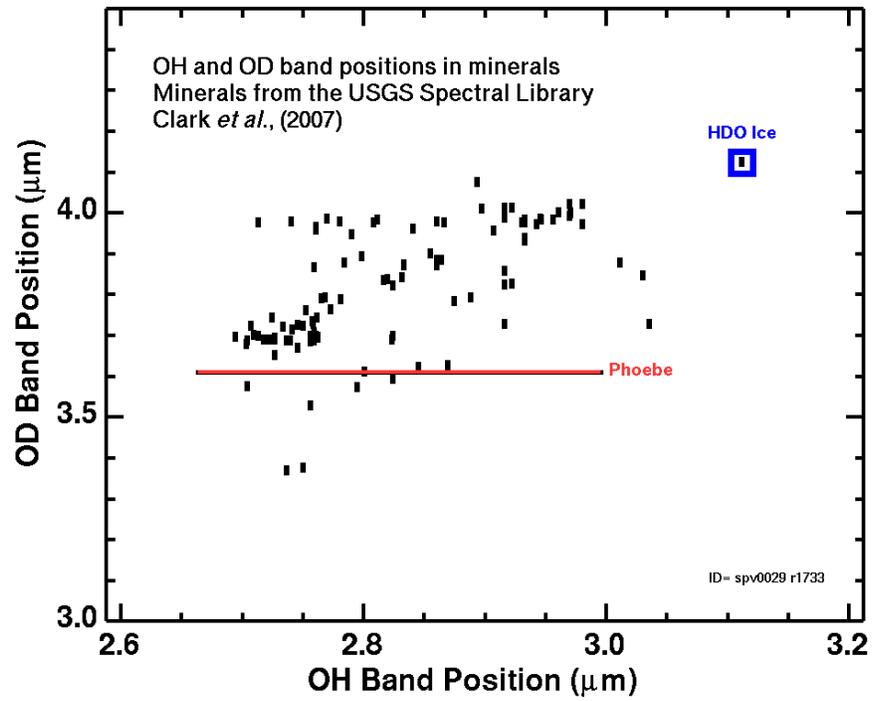
Figure 12. OD stretch band position in reflectance spectra of terrestrial minerals from the USGS spectral library 06 (Clark *et al.*, 2007). The HDO ice position is from this study.
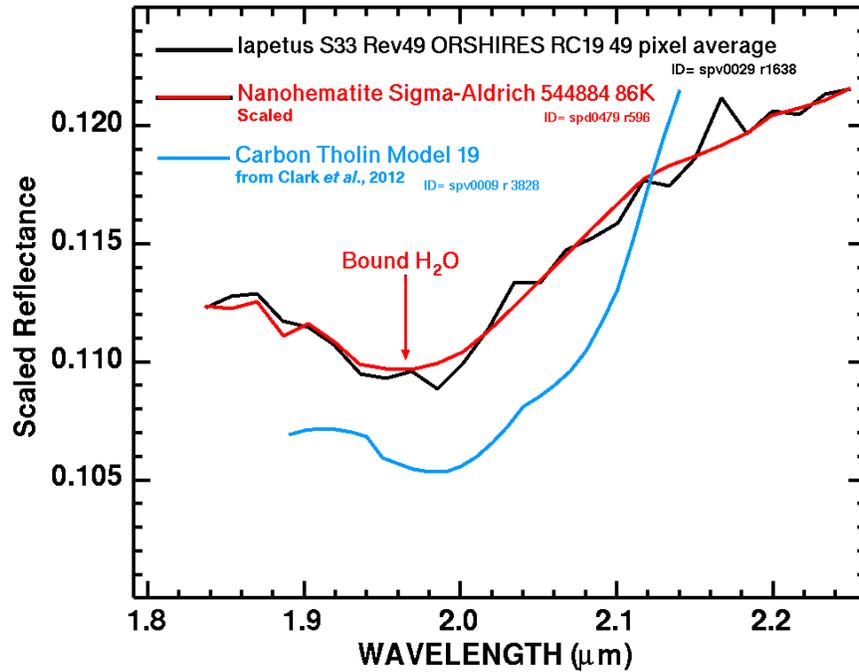
Figure 13. Spectra of a tholin and a hydrated iron oxide from Clark *et al.* (2012) are compared to the newly discovered (this study) 1.96-μm absorption feature in spectra of the Iapetus dark material. The Iapetus absorption does not match the tholin band position of this, or any other tholin for which we have observed spectrally. Post publication of Clark *et al.* (2012) the "Nanohematite" Sigma-Aldrich sample was determined to be hematite (Fe_2O_3) coated magnetite (Fe_3O_4); the water appears to be adsorbed and not structural.
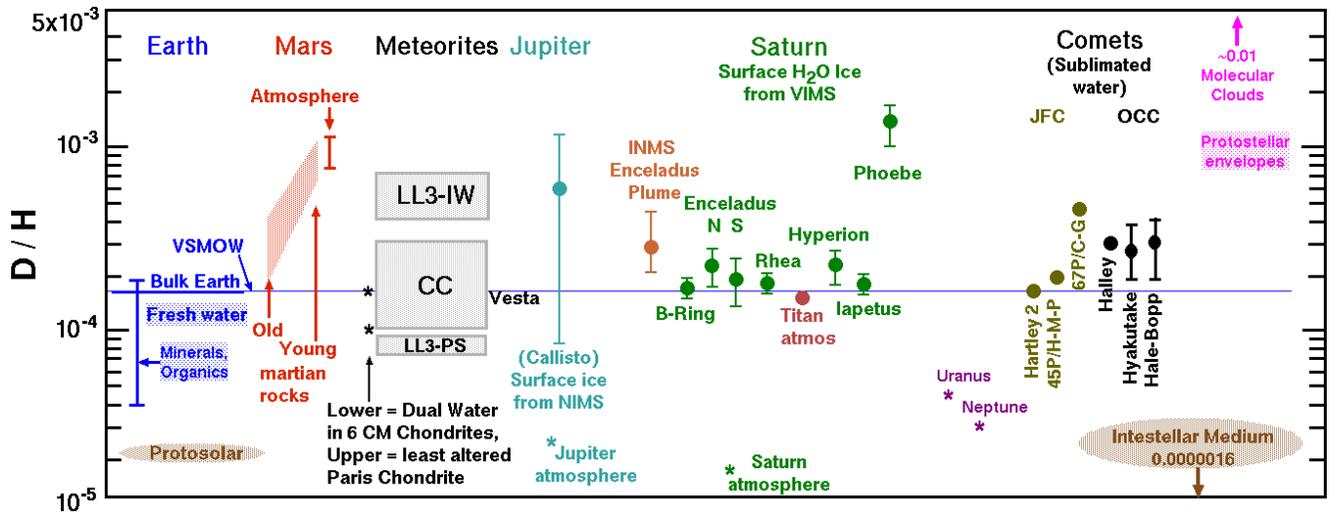
Figure 14. Measured D/H in the Solar System. Green symbols are Saturn System satellite points and Callisto: this study using NIMS data. Meteorites from Drake (2005), others as compiled by Hallis 2017 and referenced in Table 1. JFC= Jupiter family Comets. OCC= Ort Cloud Comets. The Paris CM chondrite points (i.e., black star symbols) are from Piani et al. (2018) from micro sampling 6 meteorites.
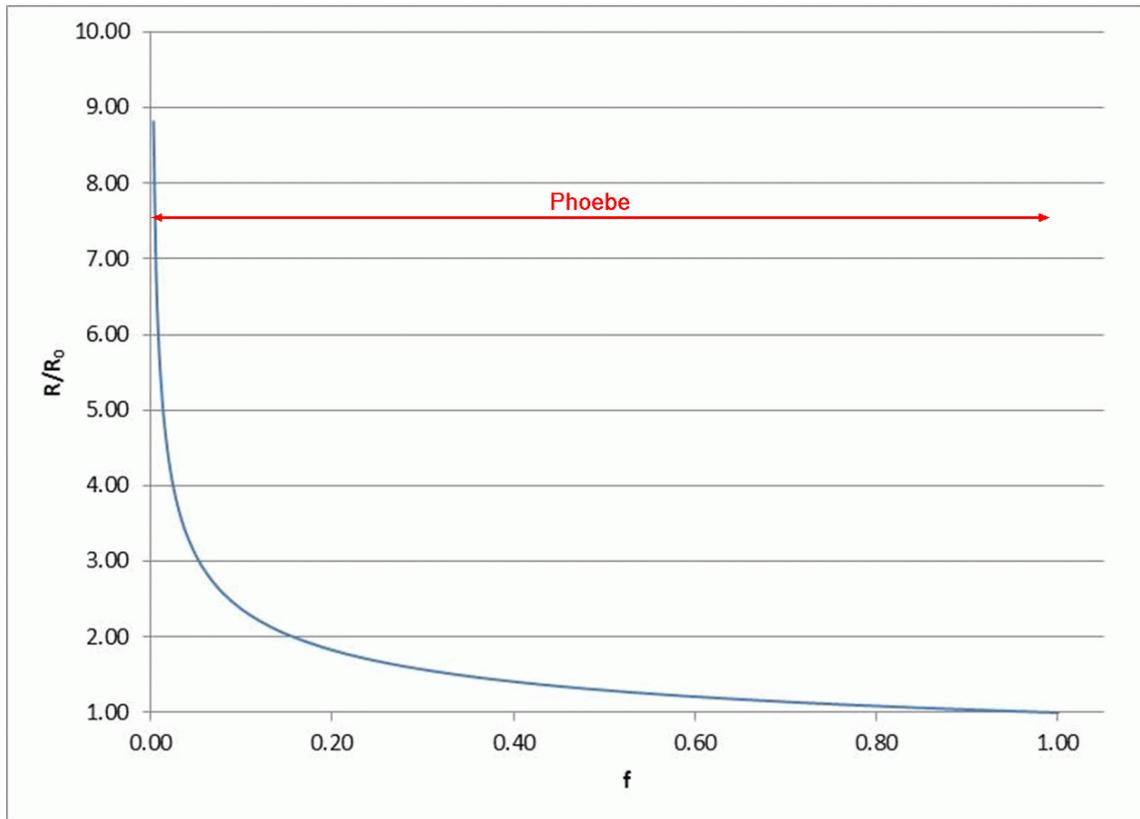
Figure 15. A Rayleigh evaporative-fractionation model. R/R_0 is the final over the initial D/H ratio, and f is the fraction of material remaining. This is a simple Rayleigh-fractionation model calculated for a well-mixed sample of water ice sublimating into a vacuum at 220 K. The 220 K temperature was chosen because models of the sublimation of comets in close proximity to the sun predict a maximum temperature of ~220 K for freely sublimating water ice in a vacuum (Fanale and Salvail, 1984, 1987 and references therein). This model is heavily idealized because it assumes that the remaining ice in the object remains well mixed, which is only possible if diffusive, downward transport of material occurs at a much higher rate than loss of material due to sublimation. In any real object this will not occur without unrealistic assumptions about downward vapor transport in porous media thus it provides a strong lower limit to the amount of material that would have to be lost to account for Phoebe's D/H by Rayleigh fractionation (red line relative to Saturn system average of D/H = 0.00017 from Table 1).